

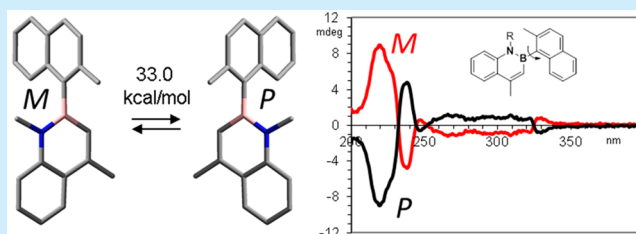
Axial Chirality about Boron–Carbon Bond: Atropisomeric Azaborines

Andrea Mazzanti, Elia Mercanti, and Michele Mancinelli*

Department of Industrial Chemistry “Toso Montanari”, University of Bologna, Viale del Risorgimento 4, I-40136 Bologna, Italy

S Supporting Information

ABSTRACT: The preparation of atropisomeric 2,1-borazaronaphthalenes is described. Resolution of the atropisomeric pair was achieved by preparative Chiral Stationary Phase HPLC (CSP-HPLC). The absolute configuration of the stereogenic axis was derived from Time-Dependent DFT (TD-DFT) simulation of the Electronic Circular Dichroism spectra (ECD). X-ray diffraction and Dynamic NMR data allowed structural and dynamic comparison with the analogue isosteric carbon compounds.



The discovery in the 20th century of biologically active axially chiral compounds useful as pharmaceutical drugs has led chemists to develop new atropisomeric compounds and to address their importance in drug discovery.^{1,2}

Dewar and co-worker proposed the first preparation of azaboraphenanthrene³ and 2,1-borazaronaphthalene⁴ where they realized the isosteric replacement of C=C with B–N within the context of an aromatic system. The forefather 1,2-azaborine was prepared only recently.⁵ This new class of compounds has attracted much attention over the past few years⁶ because of their importance in both medicinal and materials science. The replacement of two sp^2 carbon atoms by one boron and one nitrogen atom produces systems that are isoelectronic with their all-carbon analogues,⁷ yet they possess at least local dipole moments, as the N–B bond contains a significant ionic component. This polarity can significantly alter both molecular and solid-state electronic and optical properties of the system by modifying the character of the frontier molecular orbitals, and the intermolecular interactions present in solid phases.

In the recent past, we have been interested in the preparation of a new class of atropisomeric compounds bearing N–C stereogenic axes, and newly synthetic procedures of 2,1-borazaronaphthalenes⁸ stimulated our interest in the opportunity for a boron–carbon stereogenic axis able to produce thermally stable atropisomers.

In order to detect the existence of a stereogenic axis, a chirality probe is needed within the molecular scaffold. The benzylic group is well suitable to this purpose because of the isolated CH_2 that develops a simple AB-system when conformational enantiomers are formed. In this case a *p*-nitrobenzyl moiety⁹ was linked to the nitrogen of 2,1-borazaronaphthalene ring, and aromatic rings with different steric hindrances were bound to boron (compounds 1–3, Figure 1).

Single crystals of compound 1 were obtained by slow evaporation of a dichloromethane solution. Crystal structures of azaborines are rare. Seki and Hatakeyama¹⁰ reported the crystal

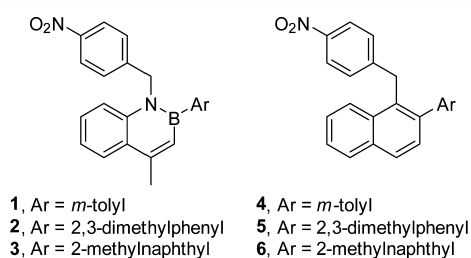


Figure 1.

structure of a B–N fused polycyclic aromatic structure where the azaborine substructure was twisted by steric interaction, reporting a B–N bond distance of 1.426 Å, typical of a B=N double bond. Most of the reported X-ray structures containing the 2,1-borazaronaphthalene ring¹¹ are $Cr(CO)_3$ complexes or contain boron–oxygen bonds. To the best of our knowledge this is the first crystal structure of a 2,1-borazaronaphthalene with both N–C and B–C bonds.¹²

A detailed investigation of the bond lengths can therefore cast new light on the electronic features of these compounds (Figure 2). The 2,1-borazaronaphthalene ring is perfectly planar and the B–N bond length is 1.427 Å, shorter than the C_4 – C_5 bond length. This confirms the strong contribution of the nitrogen lone pair to develop a double bond between nitrogen and boron. In contrast the B– C_3 bond length (1.515 Å) is more consistent with a B–C single bond, and C_3 – C_4 length is typical of an isolated C=C double bond. The structure in the solid state has the *m*-tolyl group displaced out of the azaborine plane by 72°, and the *p*-nitrophenyl group is almost perpendicular to the same plane (B–N– CH_2 – C_q dihedral angle = 104°). Due to the twisted conformation, the *m*-tolyl ring cannot develop conjugation with boron, and the B– C_q bond length is 1.581 Å.

Received: April 21, 2016

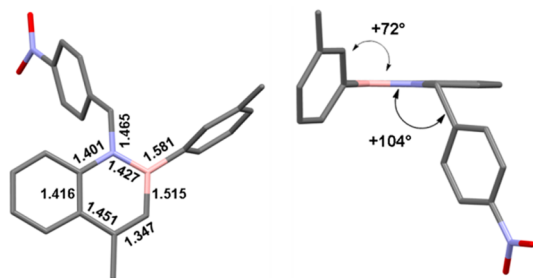


Figure 2. X-ray structure of compound **1** (crystals from dichloromethane). On the left are reported some relevant bond lengths. On the right is reported a side view showing the out-of-plane disposition of boron and nitrogen substituents. All the hydrogens are omitted for clarity.

Density Functional Theory (DFT) calculations were run¹³ at the B3LYP/6-31G(d) level of theory to explore the conformational space due to the different dispositions allowed to *p*-nitrobenzyl and *m*-tolyl rings. Four stable conformations were found, as from Figure S1 of Supporting Information (SI). They differ because of the relative disposition of the 3-methyl moiety and the benzyl moiety that can be on the same side (*syn*) or on the opposite side (*anti*) with respect to the azaborine plane. For each of the two conformations, two additional conformers are generated by a different dihedral angle of the *m*-tolyl ring (|61°| and |122°|; see Figure S1). DFT data well reproduced the ground state geometries in terms of bond distances (B–N = 1.443 Å, N–Cq = 1.404 Å, B–C₃ = 1.524 Å). Between the two available transition states for the *m*-tolyl rotation, the lowest energy one (Figure S2, top) corresponds to a rotational barrier of 6.5 kcal/mol. Albeit rather small, this barrier should be observable by the Dynamic NMR technique.¹⁴ On the other hand, two transition states were modeled and optimized also for the *p*-nitrobenzyl rotation (Figure S2, bottom). The more favorable transition state puts the two aryl rings perfectly stacked, and its energy was calculated as 10.5 kcal/mol; thus, also this conformational change could be detected by low temperature NMR.

When a sample of **1** in CD₂Cl₂ was cooled down, the CH₂ signal started to broaden below –10 °C, reached coalescence at –37 °C and eventually split into an AB-system at –89 °C (Figure 3). Line-shape simulations provided the rate constants for the rotational process, and hence the free energy of the process (10.7 ± 0.1₅ kcal/mol). This values should therefore be related to the *N*-(*p*-nitrobenzyl) rotation. On further lowering the temperature of a CDFCl₂ sample of **1**, the methyl signal of the *m*-tolyl ring broadened below –120 °C and eventually split at –150 °C into two lines with a 78:22 ratio (Δ*G*^o = 0.31 kcal/mol, Figure S3), thus confirming the formation of two conformational diastereoisomers where both rotations are frozen in the NMR time scale. Line-shape simulation provided a value of 6.6 kcal/mol for this lower barrier, in excellent agreement with the value suggested by DFT for the B-Aryl rotation (Table S1).

To unambiguously confirm which conformational process is responsible for the higher and lower barrier of compound **1**, we prepared compound **2** where the *m*-tolyl is replaced by a more hindered 2,3-dimethylphenyl ring. The presence of a methyl in the *ortho* position raises the barrier of the B-Aryl rotation, while the rotational barrier of the *p*-nitrobenzyl group should not be modified at a great extent because the 2,3-dimethylphenyl ring is parallel to the *p*-nitrophenyl ring in the transition state. DFT

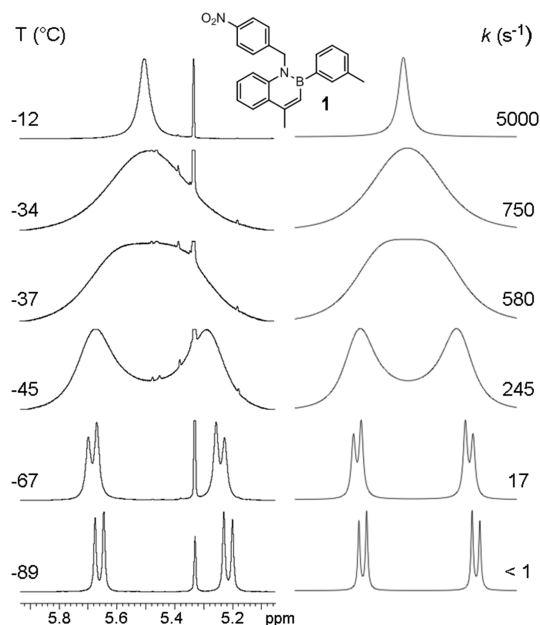


Figure 3. VT spectra for compound **1** (¹H NMR 600 MHz in CD₂Cl₂). On the left is shown the evolution of the CH₂ signal on lowering the temperature. On the right are reported the line-shape simulations with the corresponding rate constants.

calculations suggest a barrier of 16.5 kcal/mol for the B-Aryl rotation and 10.0 kcal/mol for the *p*-nitrobenzyl rotation (Figure S4).

At ambient temperature, the spectrum of compound **2** in C₂D₂Cl₄ exhibits a well resolved AB system for the benzylic CH₂, albeit with a much smaller chemical shift separation with respect to compound **1** (36 Hz for **2** and 267 Hz for **1**, respectively). On raising the temperature, the coalescence point is reached at +111 °C and a single peak is observed above +130 °C (Figure S5). The corresponding energy barrier derived from line-shape simulations is 19.1 kcal/mol. In this compound this barrier can be safely assigned to the B-Aryl rotation due to the relevant steric hindrance of the *ortho*-methyl.

When a sample of **2** in CDFCl₂ was cooled, the two doublets of the AB system broaden and split at –90 °C into two pairs of signals with a 75:25 ratio, thus confirming the formation of two conformational diastereoisomers generated by the two stereogenic axes (Figure S6). The experimental energy barrier determined by line-shape simulation was 10.0 kcal/mol, very similar to the higher barrier of compound **1** and identical to that suggested by calculations for *N*-(*p*-nitrobenzyl) rotation.

In order to compare the experimental barriers determined for B-Aryl rotation in compounds **1** and **2** with that of standard Aryl–Aryl rotation, we prepared the two naphthyl compounds **4** and **5** (Figure 1) that are the carbon isosteric analogues of **1** and **2** (see the synthetic procedure in SI). Compounds **4** and **5** were analyzed with dynamic NMR and kinetic racemization to determine the two barriers for *m*-tolyl and 2,3-dimethylphenyl rotation, which were found to be 10.7 and 25.4 kcal/mol, respectively. Rotational barriers of 8.0 and 7.6 kcal/mol were measured for *N*-(*p*-nitrobenzyl) rotation (see Figures S7, S8, S9, and S10).

The experimental data (Table 1) underline striking differences in the rotational barriers of a standard biaryl compound with respect to that of a B–C_{sp}² axis. The *m*-tolyl rotational barrier of **4** is 4.1 kcal/mol higher with respect to **1**, and that of

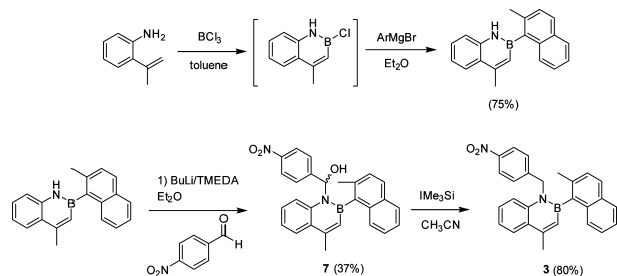
Table 1. Experimental Energy Barriers for B-Aryl and N-(*p*-Nitrobenzyl) Rotations (Energies in kcal/mol)

compd	B-Aryl	N-Benzyl	compd	C-Aryl	C-Benzyl
1	6.6	10.7	4	10.7	8.0
2	19.1	10.0	5	25.4	7.6
3	33.0	—	6	>40	—

5 is 6.3 kcal/mol higher than that of 2. In contrast, the *N*-(*p*-nitrobenzyl) rotation has a higher barrier than C_{sp²}-benzyl rotation. In the case of the B-Aryl axis this outcome could be explained by taking into account the bond distances. The experimental B-Aryl bond length is 1.58 Å while that of a standard biaryl is 1.49 Å.¹⁵ The longer distance allows better accommodation of the rotating aryl ring in the transition state. A confirmation of this hypothesis is that the difference raises when the energy barrier increases. If a conjugative stabilizing effect were present in the transition state, the rotational barrier should have the same difference upon raising the steric hindrance of the rotating ring. The same approach based on bond lengths can rationalize the different barriers observed for *N*-(*p*-nitrobenzyl) rotation. The N-CH₂ bond distance (1.46 Å) is shorter than C-CH₂ in similar compounds (1.51 Å);¹⁶ thus, compounds 1–2 exhibit *N*-(*p*-nitrobenzyl) rotational barriers higher than compounds 4–5.

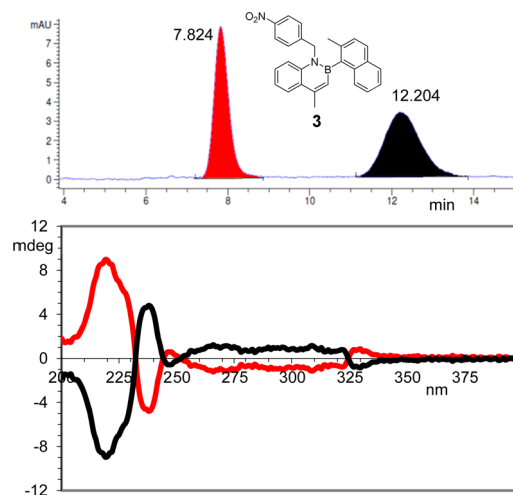
Albeit rather high, the B-Aryl rotational barrier of compound 2 does not allow for a physical resolution of the atropisomeric pair. To this aim we prepared compound 3 bearing the 2-methylnaphthalene moiety. DFT calculations suggest an enantiomerization barrier of about 31 kcal/mol for this compound (Figure S11). Taking into account the errors of calculations observed for compounds 1 and 2, the experimental barrier should be in any case larger than 25–26 kcal/mol, thus making feasible the resolution of the atropisomeric pair.

Due to the steric hindrance, compound 3 had to be prepared by means of Dewar's procedure⁴ followed by the addition of 2-methylnaphthylmagnesium bromide (Scheme 1). This inter-

Scheme 1

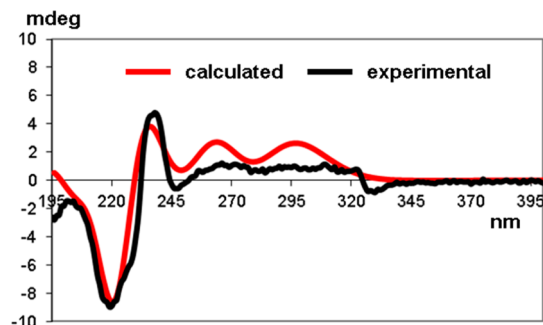
mediate was lithiated with *n*-BuLi/TMEDA and reacted with *p*-nitrobenzaldehyde to obtain compound 7 (see Figures S12–S16 in the SI for further details). The latter was effectively reduced to compound 3 with iodotrimethylsilane.¹⁷

The atropisomeric pair was resolved by means of enantioselective HPLC on a Chiralpak AS-H column, with a large separation between the two atropisomers (Figure 4, top). Good amounts of the two atropisomers were obtained by means of a semipreparative approach, and the Electronic Circular Dichroism (ECD) spectra recorded in acetonitrile showed the expected opposite traces for the two atropisomers (Figure 4, bottom). The racemization barrier was determined as 33.0 kcal/mol by keeping an enantiopure sample at +130 °C

**Figure 4.** (Top) CSP-HPLC chromatogram of compound 3. (Bottom) ECD spectra of the two atropisomers of 3, recorded in acetonitrile.

and +140 °C in C₂D₂Cl₄ and monitoring racemization by HPLC (see Figure S18).

Having in hand the two separated atropisomers of compound 3, we pursued the determination of their absolute configuration (AC) by time-dependent DFT (TD-DFT) simulation of the electronic circular dichroism spectra (ECD).^{18,19} Due to the hindered rotation of the *N*-(*p*-nitrobenzyl) group, two conformations have to be considered in the simulation of the ECD spectra. However, the exact ratio of the two conformations (50:50) can be easily determined from low-temperature NMR spectra (Figure S19) and used in the weighting of their two simulated ECD spectra (Figure 5; see SI

**Figure 5.** Comparison of the experimental ECD spectrum (black trace) of the second eluted atropisomer of 3 with the simulated spectrum (red trace) calculated at the TD-DFT CAM-B3LYP/6-311++G(2d,p) level of theory and assuming the *P* absolute configuration.

for further details). The theoretical ECD spectra were obtained using the 6-311++G(2d,p) basis set²⁰ and four different functionals (CAM-B3LYP,²¹ BH&HLYP,²² M06-2X,²³ and ωB97-XD²⁴) to allow for redundancy (see SI for further details). All the simulations assigned the *P* absolute configuration to the second eluted atropisomer of 3. Using the same approach, the absolute configuration of the atropisomers of compounds 5, 6, and 7 was determined (see SI for details).²⁵

■ ASSOCIATED CONTENT

■ Supporting Information

The Supporting Information is available free of charge on the ACS Publications website at DOI: [10.1021/acs.orglett.6b01159](https://doi.org/10.1021/acs.orglett.6b01159).

Additional Figures S1–S19; detailed procedure for the absolute configuration determination; experimental details and spectroscopic data for compounds **1**–**7** and intermediates; X-ray data for **1**; computational data for **1**–**7**; copies of ^1H , ^{13}C NMR spectra (PDF)
Crystallographic data for **1** (CIF)

■ AUTHOR INFORMATION

Corresponding Author

*E-mail: michele.mancinelli@unibo.it.

Notes

The authors declare no competing financial interest.

■ ACKNOWLEDGMENTS

The University of Bologna (RFO Funds 2013 and 2014) is gratefully acknowledged for financial support. ALCHEMY Fine Chemicals & Research (Bologna, www.alchemy.it) is acknowledged for a generous gift of chemicals.

■ REFERENCES

- (1) (a) Clayden, J.; La Plante, S. *Angew. Chem., Int. Ed.* **2009**, *48*, 6398. (b) La Plante, S. *ChemMedChem* **2011**, *6*, 505. (c) La Plante, S. *J. Med. Chem.* **2011**, *54*, 7005.
- (2) Zask, A.; Murphy, J.; Ellestad, G. A. *Chirality* **2013**, *25*, 265.
- (3) Dewar, M. J. S.; Kubba, V. P.; Pettit, R. J. *Chem. Soc.* **1958**, 3073.
- (4) Dewar, M. J. S.; Dietz, R. J. *Chem. Soc.* **1959**, 2728.
- (5) Edel, K.; Brough, S. A.; Lamm, A. N.; Liu, S.-Y.; Bettinger, H. F. *Angew. Chem., Int. Ed.* **2015**, *54*, 7819.
- (6) For reviews, see: (a) Campbell, P. G.; Marwitz, A. J. V.; Liu, S.-Y. *Angew. Chem., Int. Ed.* **2012**, *51*, 6074. (b) Bosdet, M. J. D.; Piers, W. E. *Can. J. Chem.* **2009**, *87*, 8. (c) Liu, Z.; Marder, T. B. *Angew. Chem., Int. Ed.* **2008**, *47*, 242.
- (7) Marwitz, A. J. V.; Matus, M. H.; Zakharov, L. N.; Dixon, D. A.; Liu, S.-Y. *Angew. Chem., Int. Ed.* **2009**, *48*, 973.
- (8) (a) Wisniewski, S. R.; Guenther, C. L.; Argintaru, O. A.; Molander, G. A. *J. Org. Chem.* **2014**, *79*, 365. (b) Molander, G. A.; Wisniewski, S. R. *J. Org. Chem.* **2014**, *79*, 6663. (c) Molander, G. A.; Wisniewski, S. R. *J. Org. Chem.* **2014**, *79*, 8339. (d) Molander, G. A.; Wisniewski, S. R.; Davan, E. E. *J. Org. Chem.* **2014**, *79*, 11199.
- (9) The *p*-nitrophenyl moiety was used to reduce the crowding of the aromatic region of the ^1H NMR spectrum.
- (10) Hatakeyama, T.; Hashimoto, S.; Seki, S.; Nakamura, M. *J. Am. Chem. Soc.* **2011**, *133*, 18614.
- (11) CSD search reported 23 hits using the 1,2-azaborine substructure as the input search.
- (12) Braunschweig, H.; Celik, M. A.; Hupp, F.; Krummenacher, I.; Mailänder, L. *Angew. Chem., Int. Ed.* **2015**, *54*, 6347.
- (13) *Gaussian 09 Rev. D.01*. Frisch, M. J.; Trucks, G. W.; Schlegel, H. B.; Scuseria, G. E.; Robb, M. A.; Cheeseman, J. R.; Scalmani, G.; Barone, V.; Mennucci, B.; Petersson, G. A.; Nakatsuji, H.; Caricato, M.; Li, X.; Hratchian, H. P.; Izmaylov, A. F.; Bloino, J.; Zheng, G.; Sonnenberg, J. L.; Hada, M.; Ehara, M.; Toyota, K.; Fukuda, R.; Hasegawa, J.; Ishida, M.; Nakajima, T.; Honda, Y.; Kitao, O.; Nakai, H.; Vreven, T.; Montgomery, J. A., Jr.; Peralta, J. E.; Ogliaro, F.; Bearpark, M.; Heyd, J. J.; Brothers, E.; Kudin, K. N.; Staroverov, V. N.; Kobayashi, R.; Normand, J.; Raghavachari, K.; Rendell, A.; Burant, J. C.; Iyengar, S. S.; Tomasi, J.; Cossi, M.; Rega, N.; Millam, J. M.; Klene, M.; Knox, J. E.; Cross, J. B.; Bakken, V.; Adamo, C.; Jaramillo, J.; Gomperts, R.; Stratmann, R. E.; Yazyev, O.; Austin, A. J.; Cammi, R.; Pomelli, C.; Ochterski, J. W.; Martin, R. L.; Morokuma, K.; Zakrzewski, V. G.; Voth, G. A.; Salvador, P.; Dannenberg, J. J.; Dapprich, S.; Daniels, A. D.; Farkas, Ö.; Foresman, J. B.; Ortiz, J. V.; Cioslowski, J.; Fox, D. J. Gaussian, Inc.: Wallingford, CT, 2009.
- (14) Casarini, D.; Lunazzi, L.; Mazzanti, A. *Eur. J. Org. Chem.* **2010**, *2010*, 2035.
- (15) Debeaux, M.; Brandhorst, K.; Jones, P. G.; Hopf, H.; Grunenberg, V.; Kowalsky, W.; Johannes, H. H. *Beilstein J. Org. Chem.* **2009**, *5*, 31.
- (16) Irngartinger, H.; Fettel, P. W.; Siemund, V. *Eur. J. Org. Chem.* **1998**, *1998*, 2079.
- (17) Cain, G. A.; Holler, E. R. *Chem. Commun.* **2001**, 1168.
- (18) The reference method to assign the AC relies on the X-ray anomalous scattering that in the present case would require the use of a Cu $K\alpha$ X-ray source. See: Hooft, R. W. W.; Straver, L. H.; Spek, A. L. *J. Appl. Crystallogr.* **2008**, *41*, 96–103.
- (19) For reviews, see: (a) Mazzanti, A.; Casarini, D. *WIREs Comput. Mol. Sci.* **2012**, *2*, 613. (b) Pescitelli, G.; Di Bari, L.; Berova, N. *Chem. Soc. Rev.* **2011**, *40*, 4603. (c) Bringmann, G.; Bruhn, T.; Maksimenka, K.; Hemberger, Y. *Eur. J. Org. Chem.* **2009**, *2009*, 2717.
- (20) (a) Gunasekaran, P.; Perumal, S.; Carlos Menéndez, J.; Mancinelli, M.; Ranieri, S.; Mazzanti, A. *J. Org. Chem.* **2014**, *79*, 11039. (b) Ambrogio, M.; Ciogli, A.; Mancinelli, M.; Ranieri, S.; Mazzanti, A. *J. Org. Chem.* **2013**, *78*, 3709.
- (21) Yanai, T.; Tew, D.; Handy, N. *Chem. Phys. Lett.* **2004**, *393*, 51.
- (22) In Gaussian 09 the BH&HLYP functional has the following form: $0.5 * E_X^{\text{HF}} + 0.5 * E_X^{\text{LSDA}} + 0.5 * \Delta E_X^{\text{Becke88}} + E_C^{\text{LYP}}$.
- (23) Zhao, Y.; Truhlar, D. G. *Theor. Chem. Acc.* **2008**, *120*, 215.
- (24) Chai, J.-D.; Head-Gordon, M. *Phys. Chem. Chem. Phys.* **2008**, *10*, 6615.
- (25) The reduction of a single stereoisomer of **7b** (*R,P* or *S,M*) yielded a racemic mixture of compound **3**, suggesting a fast rotation of the 2-methylnaphthyl group in the radical transition states. See: Stoner, E. J.; Cothron, D. A.; Balmer, M. K.; Roden, B. A. *Tetrahedron* **1995**, *51*, 11043. See also Figure S17 for further details.